PROCEEDINGS OF SCIENCE

LHCb Tracking, Alignment and Physics Performance

Marco Gersabeck[*†]
CERN
E-mail: marco.gersabeck@cern.ch

The LHCb experiment at the LHC is designed for precision heavy flavour physics. Its tracking, alignment and physics performance is discussed with focus on the silicon strip detectors. First results of the tracking efficiency measured with collision data are presented as well as single hit, impact parameter and vertex resolutions. The tracking efficiency is above 95% for all tracks with a transverse momentum above 100 MeV/c which covers the full physics range. The single hit resolution of the VErtex LOcator (VELO) sensors for tracks of optimal incidence is better than 4 μm for a strip pitch of 40 μm. The impact parameter resolution is found to be about 30 μm for tracks with 3 GeV/c transverse momentum. The status of the spatial detector alignment is described before discussing the proper time reconstruction performance.

19th International Workshop on Vertex Detectors - VERTEX 2010
June 06 - 11, 2010
Loch Lomond, Scotland, UK

[*] Speaker.
[†] on behalf of the LHCb collaboration.

PoS(VERTEX 2010)014

1. Introduction

1.1 The LHCb Detector

The LHCb experiment [1] at the LHC is an experiment specifically aimed at making precision measurements with heavy flavour particle decays. It has been built as a single forward arm spectrometer covering an acceptance of roughly 15 mrad to 300 mrad or from 1.9 to 4.9 in units of pseudo rapidity. This design follows the angular production of heavy flavour quark anti-quark pairs. The quark and anti-quark are predominantly produced in the same direction and close to the direction of one of the beams.

The LHCb tracking system consists of a silicon strip VErtex LOcator (VELO), a 4 Tm dipole magnet with one silicon strip tracking station (TT) before and three stations after the magnet. Each tracking stations after the magnet has silicon strip detectors in the high occupancy inner region close to the beam pipe (IT) and straw tracker modules away from the beam pipe (OT) to complete the acceptance coverage.

The LHCb detector is completed by a number of particle identification devices. Two Ring Imaging CHerenkov (RICH) detectors with a total of three different radiators allow excellent separation of pions, kaons and protons over a momentum range from 2 GeV/c to above 100 GeV/c. The calorimetry detectors comprise a scintillating pad detector for fast information in the trigger and for electron identification, a preshower detector, an electromagnetic and a hadronic calorimeter. The third set of particle identification devices are five muon stations, one of which is located upstream of the calorimeters to aid the tracking of muons and four stations downstream of the calorimeter.

The LHCb coordiate system is defined by the z axis which coincides at the nominal collision point with the axis of the beam pointing towards the rest of the LHCb spectrometer. The y axis points vertically upwards and the x axis completes the right handed Cartesian system.

1.1.1 The LHCb Silicon Detectors

The VELO consists of two halves with 42 semi circular silicon sensors each. The split into two halves allows the retraction of each half away from the beam line. This is necessary in order to protect the detector during injection of the beam into the LHC, acceleration of the beam to nominal momentum, the beam dump, and other unstable beam conditions. The retraction mechanism is described in detail in [2].

Each VELO half contains 21 modules, each of which has two sensors. One sensor on each module measures the radial coordinate (R sensor), the other one measures the angular coordinate around the beam line (Φ sensor). In addition to the 84 VELO sensors, two R sensors placed at the upstream end of each VELO half form the so-called pile-up stations. They can be used in the trigger to suppress events with very high track multiplicity or events with more than one hard interaction.

The design of the VELO is motivated by the fact that most particle tracks originate from near the beam axis. The beam axis is the symmetry axis of the detector as it is centred around the interaction region in the transverse plane at every closing. The design also allows the efficient detection of particles originating from a vertex which is displaced from that of the primary collision. This is essential in the detection of the mostly long lived heavy flavour particles.

The TT consists of four layers of silicon strip detectors, two of which measure the x coordinate and two so-called stereo layers which are rotated around the beam axis by $\pm 5^\circ$ with respect to the x measuring sensors. The IT comprises three stations of four layers each which have the same orientation as those in the TT, respectively. The silicon strip tracking stations around the magnet, TT and IT, are grouped in the silicon tracker (ST) project [3].

1.2 The LHCb Data Taking Infrastructure

The LHCb data taking chain starts with a first, hardware trigger level (L0) which operates at the LHC clock frequency of 40 MHz and reduces the event rate to 1 MHz. The L0 trigger uses as input information from the calorimeters, the muon detectors and the pile-up stations. The L0 trigger output is reduced to a rate of 2 kHz by a high-level, software trigger (HLT) operating in two stages. The first HLT stage (HLT1) aims to confirm the L0 decision using the full detector information. This is the first stage at which tracks originating from displaced vertices can be detected using information from the VELO. The second HLT stage (HLT2) performs a full track reconstruction based on a simplified geometry description and applies inclusive and exclusive event selections.

Data quality is first assessed online with a stream of about 30 kHz of events which are reconstructed in the trigger framework. A second stage of data quality assessment occurs with a dedicated stream of 5 kHz of specifically selected calibration events. Given the limited rate of this stream, these data can be reconstructed on a short time scale after they are taken. If no major problems are found the full processing proceeds, followed by a final round of checks which lead to a decision on the usefulness of these data for physics analyses.

The full offline data processing work flow has been gradually put in place and is in full operation. Data taking started with a minimal trigger. The trigger requirements are gradually tightened in order to maintain the nominal output rate of 2 kHz. During this time the more complex triggers are run in parallel such that they can be commissioned on data before operating in rejection mode.

2. Tracking

Tracking is a key component of the LHCb event reconstruction (for more details see [1] and references therein). It has to meet a number of requirements to facilitate high precision flavour physics. High efficiency is mandatory to minimise biases caused by local or global inefficiencies. The speed of both track finding and track fitting has to be optimised to allow for the reconstruction used at trigger level to be as close as possible to the offline version. Finally, high precision measurements require high precision tracking, both in terms of momentum resolution as well as position resolution in the VELO. High resolution also helps to reduce the number of reconstructed fake tracks.

Excellent momentum resolution is a cornerstone for excellent mass resolution, particularly for two-body decays, which leads to higher sensitivity in rare decay searches as well as to lower background levels in general. In the cases both of the detection of displaced vertices and of the measurement of time dependent quantities it is essential to have excellent impact parameter and vertex resolutions. The LHCb tracking is split in two stages: track finding (pattern recognition) and track fitting.

PoS(VERTEX 2010)014

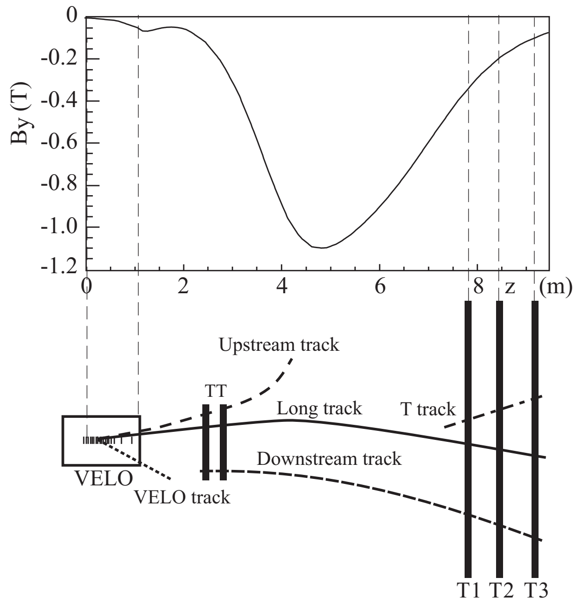

Figure 1: Vertical component of the LHCb dipole magnetic field (top) and different track types reconstructed by the tracking system (bottom). The total bending power of the magnet amounts to about 4 Tm.

2.1 Track Finding

The pattern recognition starts with a search for track seeds in the VELO. It exploits the fact that most tracks originate from somewhere close to the beam axis by only using hits on the R sensors for track finding in r-z space. A constraint in the azimuthal direction is provided by the segmentation of the R sensors into 45° sectors and used in the initial seeding stage. The search for tracks starts from the downstream end of the VELO where the hit density is lowest. A second stage uses hits on both R and Φ sensors to complement the seeds in r-z space to make 3D VELO tracks. A third step attempts to form tracks using all remaining clusters. This algorithm has no constraints on the track direction and is aimed at finding tracks which originate far from the primary collision vertex such as tracks from $\mathrm{K^0_S}$ decays.

VELO tracks are complemented with hits from the other tracking stations using two approaches to give so-called long tracks (see Fig. 1). The forward tracking extrapolates VELO tracks to the tracking stations downstream of the magnet and adds hits within a given search window. The so-called track matching attempts to combine track seeds which are independently created from hits in the tracking stations with VELO tracks by extrapolating both towards each other. Finally, hits in the TT station are added to the tracks to reduce the number of fake tracks and to improve momentum resolution.

Long tracks are the most important class of tracks for the reconstruction of physics events. However, tracks are not required to have hits in all tracking detectors as there are physics use cases where particles do not traverse the full tracking system. Decay products from long lived particles such as $\mathrm{K^0_S}$ may only be produced after the VELO and, hence, create hits only in the detectors downstream of the VELO (downstream tracks). Tracks with very low momentum may be bent by the magnetic field such that they leave the acceptance and produce hits only in the VELO and the tracking station upstream of the magnet (upstream tracks).

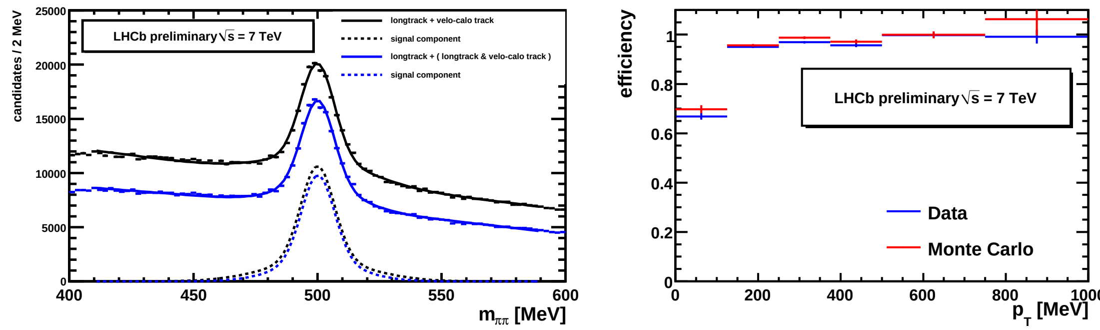

Figure 2: Efficiency of long track reconstruction using K^0_S decays. Left: Efficiency numerator (blue) and denominator (black) invariant mass distributions showing total (solid) and signal component (dashed). Right: Extracted efficiency as function of transverse momentum of the track for data (blue) and MC simulation (red).

2.2 Track Fitting

After completion of the track finding stage all tracks are fitted using a bi-directional Kalman filter. This accounts for multiple scattering in the detector material based on the particle momentum. A detailed material map is used for offline track fits. This is replaced by a simplified material map at trigger level for reasons of speed.

Spatial alignment corrections are applied in both the track finding and fitting stages, and both at trigger level and offline. The position of the two VELO halves is determined by a hardware system after each closure to an accuracy of about $5-10\ \mu$m and used to update the known alignment constants (see Sec. 3). This leads to a nominal momentum resolution of $\Delta p/p = 0.35\% - 0.55\%$ depending on the track momentum.

2.3 Tracking Performance

The performance of the LHCb tracking system and of the reconstruction software has been extensively tested with collision data.

2.3.1 Tracking Efficiencies

The efficiency of finding a particular track through the pattern recognition and successfully fitting it, is a crucial quantity. In particular, decays with a large number of daughters benefit strongly from a high tracking efficiency. There are various methods for assessing the tracking efficiency on data.

One method to measure the efficiency of finding long tracks, given that the relevant VELO track segment exists, uses the reconstruction of K^0_S candidates. The $K^0_S \to \pi^+\pi^-$ events are reconstructed from one existing long track for one of the daughters while the second daughter is reconstructed from a VELO track which points to clusters in the calorimeter. The ambiguity of clusters in the bending plane is unfolded by reconstructing the invariant mass and fitting the K^0_S peak. The efficiency of long tracks is defined by the integral of the K^0_S peak for cases where the VELO track is used in a long track which points to the calorimeter cluster normalised by the integral of the peak without the long track association. The efficiency as a function of the transverse momentum is shown in Figure 2 where the same method has been applied to simulated data for comparison. It is above 95% for all tracks with a transverse momentum above 100 MeV/c which covers the full physics range.

2.3.2 Hit Resolution & Charge Sharing

The single hit resolution of a silicon detector is the most basic quantity to assess the detector performance. It is governed by the strip pitch and the projected angle of the track producing the hit. The projected angle is defined as the component perpendicular to the strip direction of the angle between the track and a normal vector of the sensor plane. This angle strongly affects the sharing of the deposited charge between adjacent strips. Additional effects can lead to different charge sharing depending on the exact position of the track intercept between two strips. This so-called η function [4] is described in more detail below.

Another parameter which affects the hit reconstruction is the magnetic field. It leads to a bias due to a change of the drift direction of charge carriers, however it does not change the hit resolution. This bias is at the sub micron level in the VELO but is as large as 3 μm for the ST detectors (see Fig. 1 for the magnetic field strength at the position of the various detectors).

The optimal resolution for a given strip pitch is obtained for tracks which cross the width of one strip when traversing the sensor. For the VELO sensors, this optimal projected angle varies between about 7° for the innermost regions with a pitch of 40 μm, and 20° for the outermost regions with a pitch around 100 μm. For tracks at normal incidence diffusion leads to a non-zero amount of charge sharing, benefiting in particular the lower pitch regions.

Tracks with very small projected angles have different charge sharing depending on how close they are to a boundary between two strips. This dependence is described by a so-called η function which relates the dependence of the reconstructed position from the charge of the strips in a cluster to the true position given by the track intercept point. Initial studies for the VELO show a clear effect for small projected angles, whereas the charge sharing for large projected angles follows a simple weighted average of the charge of the strips involved. The use of this function as a correction to the position reconstruction is under study.

The single hit resolution has been measured using hit residuals. The distribution of these residuals is measured as a function of strip pitch for tracks in a given range of projected angles. The resolution is extracted from the width of the residual distributions by correcting for the bias which arises from the usage of the hits on the sensor under study in the track fit. Only hits other than the first and last on a track are used. Figure 3 shows the resolution for projected angles between 0° and 4° and between 7° and 11°. Already for small projected angles, the resolution is significantly better than that expected for binary readout, i.e. the pitch divided by $\sqrt{12}$. The best resolution for projected angles between 7° and 11° has been determined to be better than 4 μm for a strip pitch of 40 μm. These results are in good agreement with expectations from previous test beam experiments [5]. Some further improvement is expected from updates of the alignment which is discussed in Section 3.

Charge sharing in the ST detectors is significantly less than in the VELO due to a larger ratio of strip pitch to sensor thickness which results in almost no tracks having an angle large enough for optimal charge sharing. The charge sharing for perpendicular tracks is measured to be significantly less than what is expected from test beam results. The ST reconstruction uses η

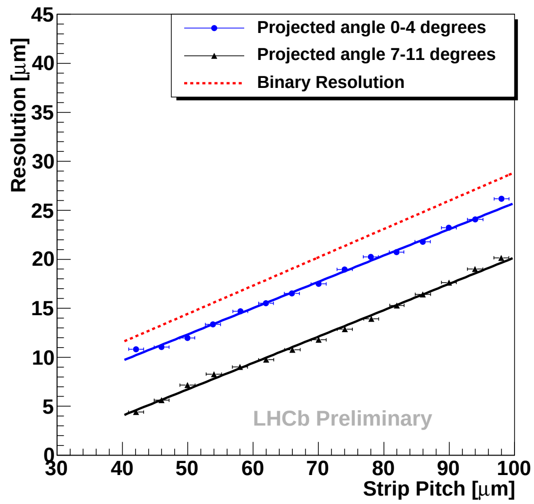

Figure 3: VELO hit resolution as function of strip pitch for different ranges of projected angle compared to binary resolution.

functions determined from data in the calculation of cluster positions. The single hit resolutions of the ST detectors are determined to be about 30% worse than expected. Significant improvements are expected from more precise alignment constants. However, about half of this discrepancy can be attributed to the difference in charge sharing at small projected angles.

2.3.3 B Tagging

The most common way to identify heavy flavour particle decays is by detecting tracks which have a large impact parameter (*IP*) with respect to the primary vertex. The *IP* is defined as the closest distance of approach between the extrapolated track and the position of the primary proton proton collision. The *IP* can be split in components by defining an x-y plane at the z location of the primary vertex and measuring the components IP_x and IP_y as the x and y intercepts of the track with the plane, respectively. For tracks originating from the primary collision point, the width of the IP_x, IP_y distributions is a convolution of the resolution in IP_x, IP_y and of the vertex resolution. The contribution from the vertex resolution is minimised by requiring a minimum number of tracks contribution to the primary vertex which effectively applies an upper limit to the vertex resolutions (see below).

The IP_x resolution obtained from first high energy collision data is about $(16+25/p_T)\mu$m (p_T in GeV/c), that for IP_y is equivalent. This means that high transverse momentum physics tracks have an IP_x, IP_y resolution of about 20 μm. The simulated resolution is significantly better at about $(11+20/p_T)\mu$m. This discrepancy led to an investigation which revealed that the RF foil, which separates the VELO sensors from the beam vacuum, was inaccurately simulated with a thickness of 250 μm instead of 300 μm. However, this correction only changed the slope of the resolution function from 20 to 21. Further investigations are ongoing to understand these differences. The measured resolution for the x and y component of the *IP* corresponds to a resolution of $(20+29/p_T)\mu$m for the full, so-called three-dimensional *IP*.

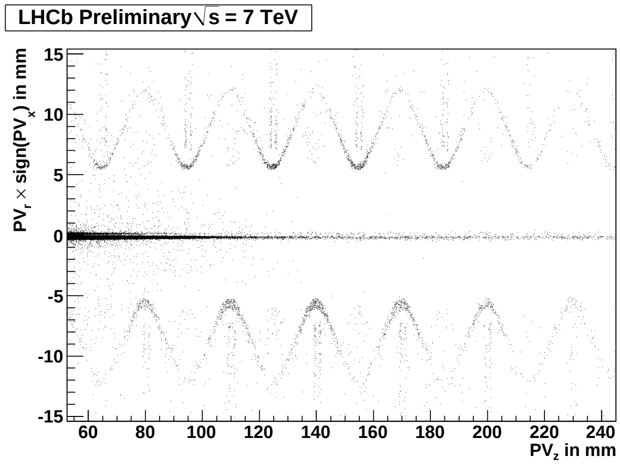

Figure 4: Distribution of vertices in the VELO region. The coordinates are the radial vertex position multiplied by the sign of the *x* position and the *z* position. The plot shows beam-gas interactions along the beam line in the centre, the sinusoidal shape of the RF foil and the sensor pairs of the VELO modules.

Improvements of the alignment are expected to account for part of the discrepancy mostly regarding the offset for high p_T tracks[1]. Additional investigations into the accuracy of the material description are under way. The currently achieved precision is already at a level which allows the full exploitation of the LHCb physics potential.

2.3.4 Vertex Resolutions

Vertex resolution is a quantity which is closely related to *IP* resolutions. Good precision on vertex resolutions is crucial for proper time reconstruction, for separating vertices from multiple interactions, and for various other quantities in the selection of physics processes. Vertex resolutions are measured by randomly splitting all reconstructed tracks in two subsets and by reconstructing vertices from each of the subsets [2]. If each of the subsets returns exactly one reconstructed vertex it is assumed that the vertices from the two subsets describe the same true interaction point. Under this assumption, the resolution can be determined from the width of the distribution of the distance between the two vertices. Following the obvious dependence of the vertex resolution on the number of tracks used in the vertex fit (N), the resolution is measured as a function of N. In the transverse plane, the vertex resolution is measured to about 78 $\mu\text{m}/\sqrt{\text{N}}$ for the *x* and *y* coordinates. In the longitudinal direction, the resolution is determined as 456 $\mu\text{m}/\sqrt{\text{N}}$. Further improvement is expected with advances on the alignment and on the calibration of the track reconstruction.

A pictorial demonstration of the vertex reconstruction quality is given in Figure 4. The plot shows the *r*-*z* position[2] of vertices that were reconstructed from three or more tracks. The horizontal line in the centre originates from beam-gas interactions, the two sinusoidal lines show interactions in the RF-foil, and the pairs of vertical lines originate from interactions in the sensor pairs of the

[1]Subsequent to the conference, alignment improvements have indeed brought good agreement between data and simulation for tracks with a transverse momentum greater than 2 GeV/c.

[2]The sign of the *r* coordinate is assigned as the sign of the *x* coordinate, following the VELO half geometry.

VELO modules. The precision of these material maps will be used to study the accuracy of the material description in detail.

3. Alignment

The alignment of the LHCb detector is a rather challenging task as the alignment precision has to be a small fraction of the respective detector resolution. The algorithms for performing the alignment are largely in place and have been presented at previous workshops [6, 7]. Initial alignment constants have been provided by a series of survey measurements of the sensitive elements of all tracking systems. There are two sets of algorithms for aligning the VELO:

- a relative alignment of the sensors based on fits to residual distributions and an alignment of the modules and the two VELO halves based on the Millepede algorithm [8, 9],
- a global χ^2 minimisation based on Kalman track fit residuals [10].

The latter approach is also used in the ST. It is complemented by a Millepede based algorithm which differs from the VELO approach by the track fit as it has to take into account magnetic field effects that are negligible in the VELO.

Compared to the other LHC experiments, LHCb could only benefit to a very limited extent from data taking with cosmic rays due to its forward geometry. However, tracks from secondary particles during LHC injection tests have been used successfully to obtain initial alignment constants, particularly for the VELO [11]. While the particle density in these tests, which was fairly uniform in the transverse plane, was low for the VELO compared to collision events, it was significantly higher for the ST. Hence, a clean track reconstruction was not possible and only a coarse alignment was achieved.

With all alignment algorithms in place, the first challenge is to distinguish real misalignment effects from those originating from other sources. In particular, the detector description can only be tested in detail with the analysis of non simulated data. Thus, an effect which appeared to be a scaling misalignment in the x coordinate of the TT has been traced down to a value of the strip pitch which was wrong by two per mille.

The main question regarding VELO alignment in the early LHC running period is the stability of the alignment over several retractions and insertions of the VELO halves. Alignment constants are measured by a hardware system and updated after each insertion at the start of an LHC fill. This relative x misalignment of the two VELO halves, i.e. in the direction of the main movement, has been found to be stable within $\pm 5\ \mu$m. This is within the required precision of the hardware alignment system.

The module and sensor alignment is known to better than 5 μm precision from an alignment obtained by studying residual distributions with data from the aforementioned injector tests. The target precision is to have misalignments below 2 μm, which is expected to be reached with completion of the analysis of first collision data.

The ST sensor alignment is at 29 μm precision for TT and 16 μm precision for IT. The target precision for both is to reach about 10 μm.

PoS(VERTEX 2010)014

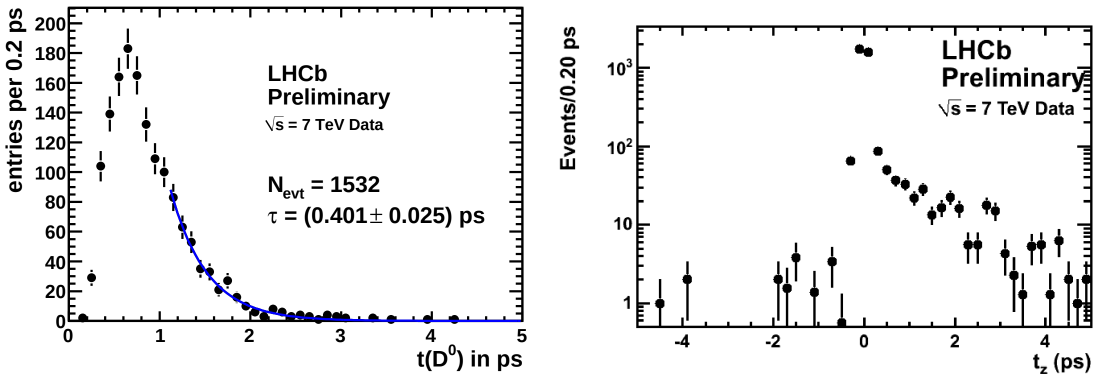

Figure 5: Left: Proper time distribution measured in $D^0 \to K\pi$ events with a fit to the region without acceptance biases. Right: Pseudo proper time distribution (taking only the *z* component of decay distance and momentum) of $J/\psi \to \mu\mu$ candidates. The narrow peak underlines the good resolution and the tail shows the presence of J/ψ from B decays.

4. Physics Performance

LHCb was commonly described during construction as a day-1 experiment. Despite the fact that the LHC operates at half its design energy this has not changed. With a total integrated luminosity of 14.4 nb^{-1} the HLT1 triggers are already operating in rejection mode, i.e. no longer accepting all events. The LHC luminosity is scheduled to approach the LHCb design luminosity to within a factor of two by the end of the year. This will require the full experiment to work close to design specifications, but also allows an early exploitation of a rich physics programme. In particular, charm physics, which benefits from looser trigger conditions, will offer a number of interesting physics opportunities as the charm production cross-section suffers the least from the lower centre-of mass energy.

The current performance of the LHCb experiment is best shown by the number of particles which have been rediscovered using the first data sample. Very clean signal peaks have emerged for all particles from pions to J/ψ. Even a first evidence of B mesons has been observed in a fully hadronic decay mode. The capability of the particle identification system is best demonstrated by the fully hadronic decays of Λ and D with reconstructed purities above 90%.

Time dependent measurements are key in heavy flavour physics. A first attempt of a lifetime measurement using $D^0 \to K\pi$ decays, performed by excluding the region at small proper times which is affected by acceptance effects, yields a value in agreement with the current world average (see Fig. 5). This shows that the momentum and vertex measurements are well calibrated within the precision of the measurement. A first estimate of the proper time resolution has been obtained from $J/\psi \to \mu\mu$ decays. Most of these are produced promptly, hence the width of their time distribution gives an estimate of the resolution (see Fig. 5). J/ψ from B decays produce a tail of positive proper time values. The lack of the same tail for negative proper times is another clear sign of the presence of B mesons in LHCb.

5. Conclusion

LHCb is a running heavy flavour experiment. It is in the transition from initial operation to detailed understanding of the detector. The tracking is fully operational and has shown very high performance from the start. Detailed studies of the efficiencies, resolutions and of the material description are under way and have already shown results which are close to expectations. The spatial alignment of the full tracking system is progressing and has proven its sensitivity to sub-micron level effects. The initial physics performance is very promising for making high precision heavy flavour measurements with early data from the LHC.

References

[1] The LHCb Collaboration, A.A. Alves Jr. et al, 2008 JINST 3 S08005.

[2] S. Redford, these proceedings.

[3] M. Needham, these proceedings.

[4] E. Belau *et al.*, Nucl.Instrum.Meth.214:253,1983.

[5] M. Gersabeck *et al.*, Nucl.Instrum.Meth.A596:164-171,2008.

[6] S. Viret, PoS(Vertex 2007)028.

[7] S. Blusk (Ed.), CERN-2007-004.

[8] S. Viret, C. Parkes, M. Gersabeck, Nucl.Instrum.Meth.A596:157-163,2008.

[9] V. Blobel, Nucl.Instrum.Meth.A566:5,2006.

[10] W. Hulsbergen, Nucl.Instrum.Meth.A600:471-477,2009.

[11] S. Borghi *et al.*, Nucl.Instrum.Meth.A618:108-120,2010.

PoS(VERTEX 2010)014